Seamless Pedestrian Navigation Methodology Optimized for Indoor/Outdoor Detection

Qinghua Zeng, Jingxian Wang, Qian Meng, Xiaoxue Zhang, and Shijie Zeng

***Abstract*— The widespread popularity of the smartphone and the increasing integrated sensors, make it possible to provide the location-based service for anyone at anytime, anywhere. The pedestrian location based on the smartphone becomes a kind of wonderful solution for indoor/outdoor positioning. A smartphone fusion location method optimized by the indoor/outdoor detection is proposed in this paper. The light sensor signal, the magnetic sensor signal, and the global navigation satellite system (GNSS) signal are integrated into the navigation algorithm to improve the accuracy of the location identification. When the device is detected indoors, the pedestrian dead reckoning algorithm based on the accelerometers and gyroscopes is applied, the initial location and the heading direction values are obtained with the help of the mobile image sensor and the indoor electronic map. When the device is detected outdoors, the GNSS and the magnetic sensor are introduced in the system to assist the inertial process of the navigation. The experiment results indicate that the continuity and the accuracy of the seamless position between the two environments are effectively improved. It is a no-blind area indoor/outdoor navigation with the help of the indoor/outdoor detection method proposed in the paper.**

***Index Terms*— Pedestrian navigation, multi-information fusion, indoor/outdoor detection, seamless position.**

I. Introduction

With the development of the smartphone and the rich MEMS (Micro-electromechanical Systems) sensors, the pedestrian navigation and the positioning technology based on the smartphone become an important emerging branch in the navigation area. The smartphone navigation system can be used to calculate the position of the pedestrians and to monitor the motion of the human body. It can be used in kinds of applications in military and civilian [1]–[3]. The urbanization is getting faster and faster in the contemporary society, there are many new requirements for the indoor/outdoor integrated navigation. The pedestrian location based on the smartphone becomes a feasible solution for the two environments navigation.

At present, the research directions are mainly concentrated in two relatively independent fields: the indoor positioning methods and the outdoor positioning methods.

Manuscript received July 21, 2017; accepted September 26, 2017. Date of publication October 20, 2017; date of current version December 7, 2017. This work was supported in part by the National Natural Science Foundation of China under Grant 61533008, Grant 61374115, and Grant 61603181, in part by the Fundamental Research Funds for the Central Universities under Grant NJ20170005 and Grant NJ20170010, and in part by the Priority Academic Program Development of Jiangsu Higher Education Institutions. The associate editor coordinating the review of this paper and approving it for publication was Prof. Giancarlo Fortino. *(Corresponding author: Qinghua Zeng.)*

The authors are with the Navigation Research Center, Nanjing University of Aeronautics and Astronautics, Nanjing 211106, China (e-mail: zengqh@nuaa.edu.cn; nrcwjx@nuaa.edu.cn; mengqian@nuaa.edu.cn; zhangxiaoxue@nuaa.edu.cn; zengshijie@nuaa.edu.cn).

Digital Object Identifier 10.1109/JSEN.2017.2764509

The radio frequency technology, the micro inertia and the other sensors are used together for indoor positioning information [4]–[6]. The PDR method is one of the most widely methods used indoors. Wei Chen, et al presented three typical step length estimation models and a unified heading error model in order to improve the PDR accuracy [7]. Wonho Kang and Youngnam Han proposed a new algorithm to find a reasonable heading direction by using the measurements from the magnetometer and the gyroscope together [3]. WIFI (Wireless Local Area Net based on 802.11 standards) is another typical localization method [8]–[10] in the indoor environment.

The GNSS/GPS (Global Position System) and micro inertia sensors have been used together in the outdoor positioning technology. Lots of methods, such as the de-noising INS (Inertial Navigation System) signals and the precise point positioning of GNSS are used in the outdoor environment. Wonkyo Seo, et al utilized the UPF (Ultraviolet Protection Factor) to filter the noise caused by the acceleration, deceleration, and unexpected slips. The noise of the internal INS sensors [11] is reduced. Lina Zhong proposed an INS/SFGPS-PPP tightly-coupled navigation system and a robust adaptive filtering method based on the dynamic cycle slip compensation [12].

For the purpose of realizing the overall seamless navigation, Jiantong Cheng proposed an integrated navigation system, which can be used for the pedestrian inertial navigation in the outdoor/indoor environments with the aid of WIFI and GNSS [13]. Yoshihiro Sakamoto, et al presented an indoor/outdoor seamless robot navigation method by using pseudo-satellites and the indoor messaging system [14].

In order to improve the overall availability and autonomy of indoor/outdoor pedestrian navigation, a smartphone fusion location method optimized by indoor/outdoor detection is very important and necessary. Oscar Canovas, et al presented a binary classifier, based on AdaBoost, which made use of the WIFI signals in order to infer the indoor/outdoor condition [15]. The research work [16], [17], introducing the MEMS sensors in the transition zone between the two environments, gave a glimmer of hope to realize a seamless indoor/outdoor navigation.

Indoor facilities, such as the WIFI and the pseudo-satellites, are mainly used in the identification of indoor/outdoor environments to achieve the better seamless positioning performance. To develop the independent indoor/outdoor seamless navigation algorithm, the combination of multiple sensors in the smart phone can be applied to deal with the environments discrimination.

A method based on the self-contained sensors of the smartphone was studied and implemented in this paper. The light sensor, the magnetic sensor and the GNSS module of the smartphone are used to identify the indoor/outdoor environment. Then, the corresponding navigation algorithm is proposed to realize the identification function. Compared with the identification method of the GNSS, the efficiency of the identification method in this paper is improved. The magnetic sensor, the inertial sensors and the GNSS are used in fusion positioning outdoors. As to the indoor positioning, the PDR navigation method based on the MEMS accelerometers and gyroscopes is applied. The initial position and the attitude parameters can be obtained from the combination of the mobile image sensor and the indoor electronic map.

A real-time android platform for smartphone is designed and implemented based on Baidu Map SDK (a Map Software Development Kit from Baidu Company). Baidu Map is a similar product as Google Map, and Baidu Map is convenient to be used in China. The navigation results, such as the position, velocity and attitude values, can be obtained and displayed with the map. At the same time, these data can be stored into a specific database for the track reproduction. The experimental results indicate that the method proposed in the paper has a wonderful performance for the future application.

II. Indoor and Outdoor Environmental Identification Strategies

The automatic switch of the indoor/outdoor location mode is very useful in the seamless location. Some localization patterns for these two environments are applied to identify the pedestrian environment with the machine learning idea [18], [19] and the fused method [20] etc. Considering the time delay and the power consumption, it is very hard to detect the indoor/outdoor environments with only GPS receiver [21], [22] is inefficient. The output data of the light sensor and the magnetic sensor show some regularity when the environment changes. These sensors can be used for indoor/outdoor environment identification. Comprehensive environment identification method with high precision can be achieved with the fusion status of these sensors. The environment identification algorithm based on the light sensor, the magnetic sensor and the GNSS receiver is as follows.

A. Indoor and Outdoor Environmental Identification Algorithm Based on Light Sensor Information

The sunlight is the major light source in outdoor environment during the daytime. The sunlight intensity is stronger than that of the indoor artificial light. The indoor light intensity is significantly lower than the outdoor light intensity. The obvious differences of the indoor/outdoor brightness can be used to provide a foundation for two environments identification. If the smartphone is put into the pocket or the surface of smartphone is covered, the output of the light sensor cannot detect the true light intensity of the environment. In this paper, the distance sensor of the smartphone is also used to judge whether there is a cover near the smartphone. If the output of distance sensor is greater than 0, the light sensor is available. If the output of distance sensor is constant 0, it means the smartphone is covered, and the light sensor is not available.

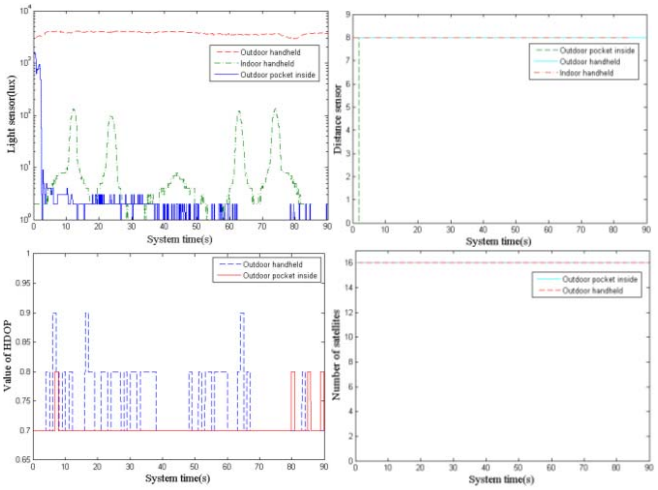

Fig. 1. Light sensor, distance sensor and GNSS output under different situation.

In order to measure the light intensity in these two environments, many experiments have been carried out under four kinds of different situations in this paper. The light intensity data of the indoor/outdoor environment are collected when the smartphone is in the pocket or in the hand. The data of all the sensors are collected at the same time.

As shown in Fig. 1, when the smartphone is hold in the hand under the outdoor situation, the output of the distance sensor is 8, which means that the light sensor is available. The light intensity is more than 2000lux. The number of the GNSS satellites is more than 10, and the HDOP (Horizontal Dilution of Precision) value is less than 1. When the smartphone is put in the pocket under the outdoor situation, the output of the distance sensor is 0, which means that the light sensor is unavailable. The light intensity is zero. The GNSS signal output can be used for indoor/outdoor environmental identification. Under the indoor handhold situation, the output of light sensor is lower than 150lux, and the GNSS signal is unavailable indoors.

Generally, the light intensity of the outdoor environment is more than 2000lux and the indoor light intensity is no more than 300lux. The light intensity is relatively stable in both environments, this characteristic can be used to distinguish between indoor and outdoor environment. Experiments results indicate that the light sensor data can be used to check the indoor and outdoor environment status clearly. While the smartphone is moved out of the building, the data of light sensor increases significantly. Lots of experiments indicate that 500lux can be chosen as the threshold to divide the indoor and outdoor environment. Therefore, the value of the light sensor can be used in automatic switching for indoor and outdoor location mode.

B. Indoor and Outdoor Environment Recognition Algorithm Based on Magnetic Sensor Information

Considering the electromagnetic environments are different, the data characteristics of the magnetic sensors under these two

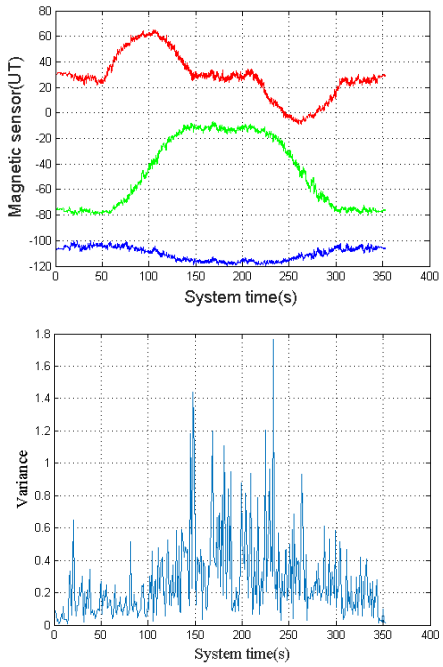

Fig. 2. The outdoor output of the magnetic sensors and the total variance.

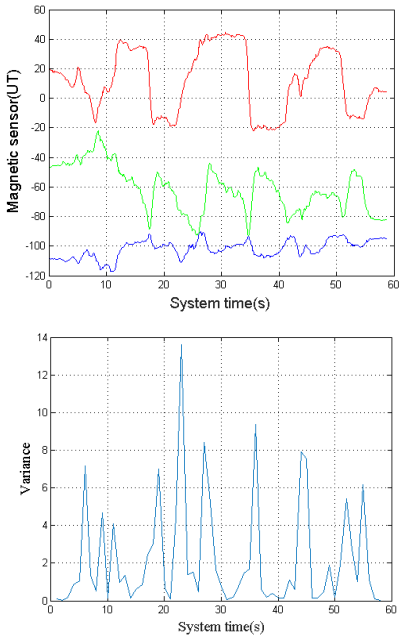

Fig. 3. The indoor output of the magnetic sensors and the total variance.

situations are different. With the help of the characteristics of the magnetic signal, two environments can be distinguished. The magnetic sensor information was collected in the indoor/outdoor environments. The curves of the magnetic sensors information and their total variance per second in the different environments are plotted in Fig. 2 and Fig. 3 respectively.

Comparing the curves of the magnetic sensors, we can easily find that the total variance value of the magnetic sensors is different. For the complex building structure and the electrical

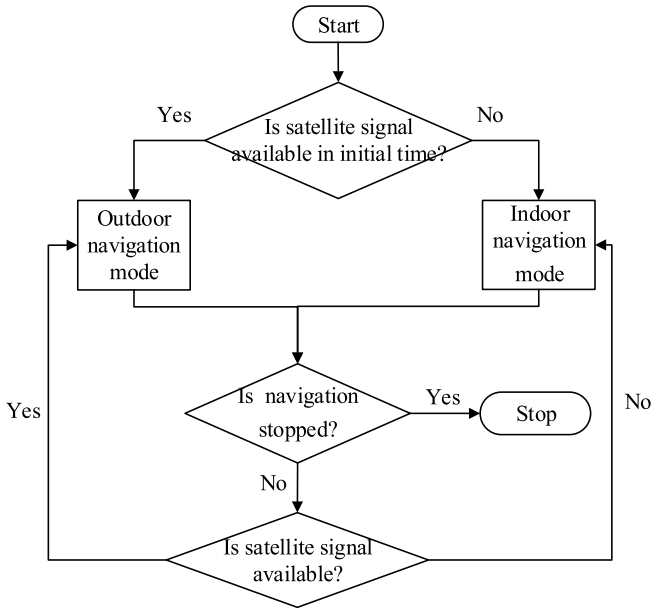

Fig. 4. Schematic diagram of the location mode switching strategy based on satellite signal recognition.

equipment indoors, the indoor magnetic variance changes more violent than the outdoor magnetic variance.

Generally, the total variance of the magnetic sensor per second has smaller output noises under the outdoor situation. The value of the total variance is less than 3. The variance of the magnetic sensor has the greater noises under the indoor situation. The value of the total variance is more than 5. The empirical results indicate that 4 can be used as a suitable threshold to discriminate the indoor and outdoor environments.

C. Indoor and Outdoor Environment Recognition Algorithm Based on Satellite Signal

The GNSS signal is unavailable in the buildings. It can be used to determine the environment of the smartphone. In general, the validity of the GNSS signal is judged by the satellite number and the HDOP value. In this paper, combined with the characteristics of pedestrian navigation, three aspects have been mentioned to verify the GNSS signal:

(1) Whether the GNSS received signal is valid;

(2) Whether the HDOP and the number of satellites satisfy the conditions: HDOP$<$3 (the empirical value) and the satellite number $>=$4 (The positioning algorithm requires 4 satellites at least);

(3) Whether the GNSS positioning result is within the distance limitation of the human walking. The distance obtained from the continuous GNSS signal should be limited according to the walking speed of the pedestrian. Considering the influence of the noises, the distance within 1 second should less than 3 meters. This value is useful for the walker, and it should be greater if it is used for the runner.

As shown in Fig. 4, the positioning mode of the system is selected at the beginning by determining the availability of GNSS signals. In the process of navigation, the indoor and the outdoor mode will be switched based on the real-time judgment result of the GNSS signal.

D. Indoor and Outdoor Environment Recognition Algorithm Based on the Light/ Magnetic / Satellite Information Fusion

Former indoor/outdoor environment recognition algorithms, based on light sensor, magnetic sensor and GNSS signal separately, can obtain the environment recognition result, but they have following drawbacks:

(1) The distance sensor in the smartphone should be used to determine whether the light sensor is covered in the daytime. The light sensor cannot be used for indoor and outdoor environment recognition when it is covered.

(2) The magnetic sensor is easily affected by the nearby electronic equipment. It might report the wrong environment result.

(3) The GNSS information of smartphone has some delay compared to the changing environments.

Therefore, it is necessary to study a kind of light/magnetic/satellite information fusion algorithm for accurate and real-time indoor/outdoor environment recognition. The loose judgment of the indoor/outdoor determination method will lead to the large errors, which will affect the positioning accuracy and navigation stability. In this paper, a "And" logical judgment has been used in indoor/outdoor environment recognition algorithm based on the light/magnetic/satellite information fusion. The outdoor mode will be determined only when all available sensors indicate this mode. The information of the satellite and magnetic sensors will be introduced into the extended Kalman filter data fusion processing to reduce the positioning error.

The results of the indoor/outdoor environment recognition algorithm based on the light/magnetic/satellite information fusion should be deduced carefully. Firstly, four situations can be divided into two groups by judging the satellite signal and the light sensor signal. Then, a comprehensive judgment can be obtained according to the recognition results of each module. The specific fusion strategy is shown as Table I.

In the table I, G(), L() and M() represent the results of the indoor/outdoor environment recognition method based on the GNSS, the light sensor and the magnetic sensor respectively. 1 means outdoor status and 0 means indoor status. Comprehensive results represent the identification result based on the light/magnetic/satellite information fusion.

In order to verify the effectiveness of this algorithm, many experiments have been carried out with the smartphone in the College of Automation engineering, Nanjing University of Aeronautics and Astronautics. During the experiments, the light sensor, the distance sensor, the magnetic sensor and the satellite module in the smartphone are all turned on to collect the data at the same time. Researcher walks into and out of the building in turn. One of the results is shown as Fig. 5. Each module can achieve indoor/outdoor environment recognition result. When the data of the sensors satisfy their corresponding threshold, the researcher can be considered in/out of the building. Considering the light sensor and GNSS module cannot be available all the time. The variance of the magnetic sensor may cause erroneous judgment due to the indoor electromagnetic equipment interference. As we know, it's a miscarriage of justice from M2 to M3 in Fig. 5 (b).

TABLE I

DECISION TABLE FOR INDOOR/OUTDOOR ENVIRONMENT BASED ON LIGHT/MAGNETIC/SATELLITE INFORMATION FUSION

Whether the satellite is available	Whether the light sensor is available	The results of each module	Comprehensive results (outdoor 1,indoor 0)
√	√	G(1)，L(1)，M(1)	1
		Other	0
	---	G(1)，M(1)	1
		Other	0
---	√	L(1)，M(1)	1
		Other	0
	---	M(1)	1
		M(0)	0

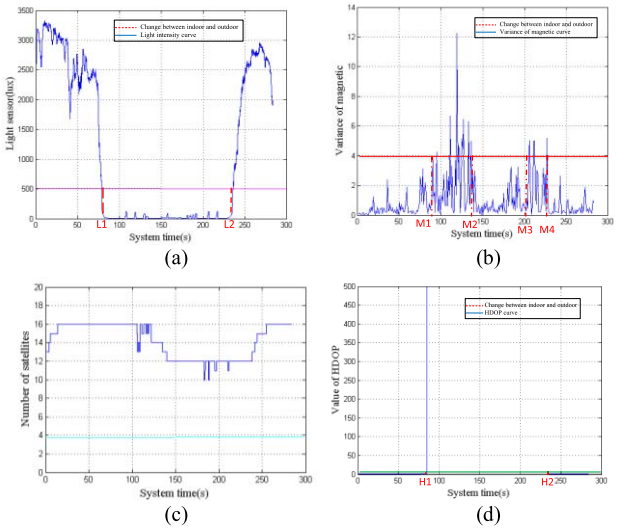

Fig. 5. Environment characteristic change of indoor/outdoor environments.

The indoor and outdoor environment recognition algorithm based on the light/magnetic/satellite information fusion proposed in this paper can avoid the former problems. Fig. 6 is the comprehensive results of these sensors. The identification result of the light sensor and the magnetic sensor are shown with the dotted line and the broken line separately. The blue solid line represents the identification result of GNSS. 1 means outdoor status and 0 means indoor status. The heavy black line represents the comprehensive identification result. To avoid the coincidence of the curves, 0.5 means outdoor status and −0.5 means indoor status. The correct indoor situation is recognized within the time span between T1 and T2.

III. INDOOR NAVIGATION MODE

The initialization parameters are the necessary values for the inertial integration navigation algorithm [23]. Considering the low-cost MEMS sensors of the smartphone, the positioning error of the smartphone is accumulated with the time [24], [25]. As we know, the pedestrian dead reckoning algorithm is one of the navigation methods, the step frequency and the step length can be estimated based on the human body motion model [26]. Bases on the dead reckoning algorithm in

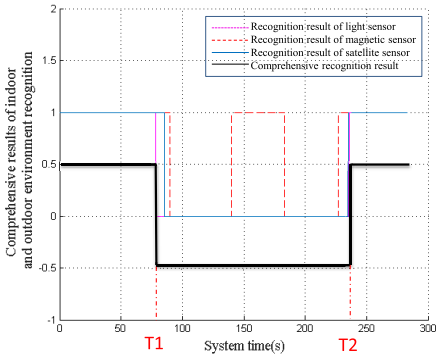

Fig. 6. Comprehensive results of the indoor/outdoor environment recognition based on the light/magnetic/satellite information fusion.

this paper, the optimized indoor navigation program is realized with the smartphone built-in IMU (Inertial Measurement Unit). Acquiring the initial position and the initial heading information in combination with the mobile image sensor and the indoor electronic map is a special process in the paper.

A. Acquisition of the Initial Position and Initial Heading

1) Text Recognition Software for the Smartphone Photo: The software, which can take pictures, store photos, identify the text in the picture, is realized in the android smartphone. The text recognition OCR (Optical Character Recognition) technology is used in the software to identify text in the photo taken by smartphone camera. These texts are valuable aid information for the indoor navigation of the smartphone.

2) Acquisition of Initial Position and Initial Heading: Before the start of the navigation, the pedestrian takes a picture of the door number at the starting point. With the help of the text obtained from the photo, the initial position information can be recognized and matched with the indoor map database. The initial geographical coordinates of the corresponding position can be determined.

The pedestrians generally walk on the right side of the road in China mainland, which means that the door number on the right side can be easily captured. The initial heading can be determined by combined with the direction of the corridor according to the indoor map database.

During the indoor walking process, many environmental characteristics points indoors can be visual captured. The visual navigation method is introduced to assist the acquisition of the navigation information of the position and the heading of the inertial navigation.

B. IMU Pedestrian Dead Reckoning Algorithm

After the acquisition of initial position and initial heading information, the pedestrian location can be calculated by the sensor data of smartphone according to the PDR principle in Fig. 7. E is the eastward position, N is the northward position. At the initial moment t_0, the original position of the pedestrian is (E_0, N_0). S_0 is the distance, θ_0 is the direction. The new pedestrian position is (E_1, N_1) at the next moment t_1. Analogously, the location of the pedestrians can be calculated

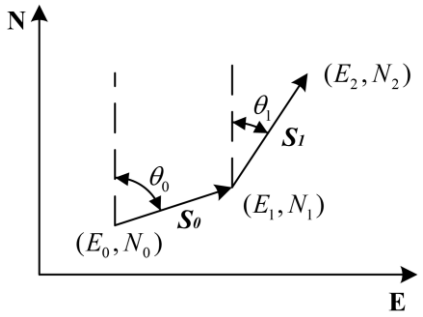

Fig. 7. Algorithm schematic of PDR.

by equation (1) at any time. The accuracy of PDR depends on step counting, heading information and step length.

$$E_k = E_0 + \sum_{i=0}^{k-1} S_i \sin\theta_i$$
$$N_k = N_0 + \sum_{i=0}^{k-1} S_i \cos\theta_i \quad (1)$$

1) The Step Counting Algorithm: The step counting algorithm is divided into three categories: the peak detection, zero crossing detection and flat zone detection. The first two detections are used to count the steps by detecting the special value of acceleration. Considering the real-time requirements of the smartphone in the paper, the peak detection method is chosen for the step-counting algorithm.

During the walking process, the vertical acceleration increases and decreases within one-step cycle. Therefore, the rising or falling interval of Z-axis acceleration can be used to count the steps. Although the original Z-axis accelerometer output has a certain periodicity, it is affected by the noises. The output period of the Z-axis is hard to be used to calculate the steps directly. Its signals need to be filtered to eliminate the noises as much as possible.

The step frequency of the human is about 1∼3 steps per second. The frequency of the useful signals in original signals is between 1 to 5 Hz. To eliminate the signal noise, band-pass filter was designed to retain the useful signal. The digital FIR (Finite Impulse Response) band-pass filter is used to extract the useful signals, and the result is shown in Fig. 8. The characteristic of the vertical acceleration in step cycle is as following:

1. Under most circumstances, the maximum and minimum values of acceleration appear only once in a step cycle and it has one rising interval and one falling interval. But some step cycle has two pairs of extreme point, so it has two rising intervals and two falling intervals.

2. Each monotone range (rising or falling) should be half of the step cycle, which continues between 0.2 to 1 second. The duration of the monotone interval is between 0.1 to 0.5 seconds. If the sampling frequency is 50Hz, each monotone interval has 5 to 25 sampling points.

3. After eliminating the noise influence, the maximum and minimum values of the acceleration are not less than 0.5 m/s^2.

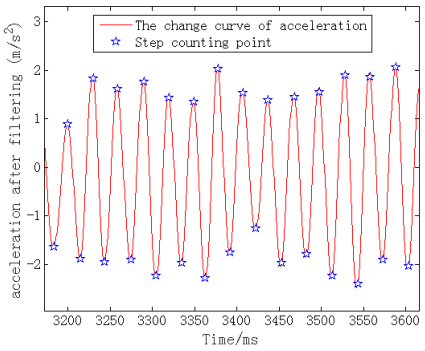

Fig. 8. Z-axis accelerometer output after filtering.

The steps can be counted by using the following formula:

$$\begin{cases} peak = \left| Acc_z^{new} - Acc_z^{old} \right| \\ stepcount = stepcount + 0.5 thr_{\min} < peak < thr_{\max} \\ stepcount = stepcount \text{others} \end{cases} \quad (2)$$

Where, *peak* is the absolute value of the difference between two adjacent peaks, Acc_z^{new} is the peak of the acceleration at present, Acc_z^{old} is the peak of the acceleration at the previous moment, *thr* is the threshold range, *stepcount* is the pedometer variables.

2) Heading Angle Correction Algorithm: The gyroscopes can be used to calculate the attitude angles. It has high precision within a short time. During the walking process, the gyros outputs will be affected by the body swings. To get a good result, the mean of the gyro output is obtained per second. The quaternion is used to realize the real-time navigation solution in the smartphone.

The initial value of the quaternion ($q(t)$) is determined by the system attitude angle (the heading angle ψ, the roll angle ϕ, the pitch angle θ) at the initial moment.

$$q(t) = \begin{bmatrix} q_0(0) \\ q_1(0) \\ q_2(0) \\ q_3(0) \end{bmatrix} = \begin{bmatrix} \cos\frac{\psi_0}{2}\cos\frac{\theta_0}{2}\cos\frac{\phi_0}{2} + \sin\frac{\psi_0}{2}\sin\frac{\theta_0}{2}\sin\frac{\phi_0}{2} \\ \cos\frac{\psi_0}{2}\cos\frac{\theta_0}{2}\sin\frac{\phi_0}{2} - \sin\frac{\psi_0}{2}\sin\frac{\theta_0}{2}\cos\frac{\phi_0}{2} \\ \cos\frac{\psi_0}{2}\sin\frac{\theta_0}{2}\cos\frac{\phi_0}{2} + \sin\frac{\psi_0}{2}\cos\frac{\theta_0}{2}\sin\frac{\phi_0}{2} \\ \sin\frac{\psi_0}{2}\cos\frac{\theta_0}{2}\cos\frac{\phi_0}{2} - \cos\frac{\psi_0}{2}\sin\frac{\theta_0}{2}\sin\frac{\phi_0}{2} \end{bmatrix} \quad (3)$$

The angular outputs of the IMU ($\omega_{nbx}^b, \omega_{nby}^b, \omega_{nbz}^b$) are used to renew the quaternion correction.

$$\begin{bmatrix} \dot{q}_0 \\ \dot{q}_1 \\ \dot{q}_2 \\ \dot{q}_3 \end{bmatrix} = \frac{1}{2} \begin{bmatrix} 0 & -\omega_{nbx}^b & -\omega_{nby}^b & -\omega_{nbz}^b \\ \omega_{nbx}^b & 0 & \omega_{nbz}^b & -\omega_{nby}^b \\ \omega_{nby}^b & -\omega_{nbz}^b & 0 & \omega_{nbx}^b \\ \omega_{nbz}^b & \omega_{nby}^b & -\omega_{nbx}^b & 0 \end{bmatrix} \begin{bmatrix} q_0 \\ q_1 \\ q_2 \\ q_3 \end{bmatrix} \quad (4)$$

The direction cosine matrix between the carrier coordinate system and the geographic coordinate system is solved as follows:

$$C_n^b = \begin{bmatrix} 1-2(q_2^2+q_3^2) & 2(q_1q_2+q_0q_3) & 2(q_1q_3-q_0q_2) \\ 2(q_1q_2-q_0q_3) & 1-2(q_1^2+q_3^2) & 2(q_2q_3+q_0q_1) \\ 2(q_1q_3+q_0q_2) & 2(q_2q_3-q_0q_1) & 1-2(q_1^2+q_2^2) \end{bmatrix} \quad (5)$$

The heading angle ψ, in the equation (6), can be obtained from the components of the equation (5), and it can be shown as:

$$\psi = \arctan\left(\frac{C_{12}}{C_{11}}\right) \quad (6)$$

In this paper, the pedestrian walking is divided into two modes: straight and turn. The specific formula is as follows:

$$\begin{cases} \psi_{now} = \psi_{before} + \omega_z^- * T & \omega_z^- > thr \\ \psi_{now} = \psi_{before} & others \end{cases} \quad (7)$$

Where ψ_{now} is current heading, ψ_{before} is the heading of the last moment, ω_z^- is average of gyro Z-axis output per second, T is the sampling period, *thr* is the threshold of turn judgment. ω_z^- and *thr* are used to determine the turning status of the pedestrian.

From the Fig. 9 and Fig. 10, there are four turns during walking process. The change of the heading angle of each turn is about 90 degree. The curve peak of average angle velocity is corresponded with the turning process. The integral value

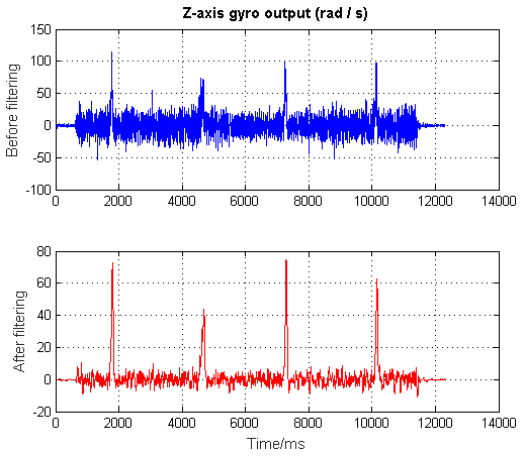

Fig. 9. Gyroscope output before and after average process.

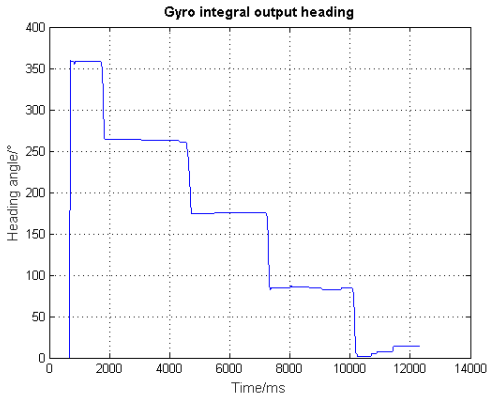

Fig. 10. Heading angle changing by gyroscope output.

TABLE II
COMPARISON OF GNSS STEP SIZE AND ACTUAL STEP SIZE

	Steps	Distance	Step length
Test results	1234	1004.58m	0.814m
Actual results	1236	1000.24m	0.809m
Error	0.16%	0.43%	0.618%

of the gyroscope output is substantially equal to the turning angle. Thus, it can effectively eliminate the influence of the body swing and obtain the accurate heading angular rate.

3) Calculation of Step Length: In this paper, GNSS calibration method is used to calculate the step length of pedestrian. The step length is equal to the distance divided by the number of steps. The pedestrian step length is measured in the open place, and the average step length can be obtained to analyze the error performance. The actual step length is calculated with the help of the centimeter-level differential GNSS system. As shown in Table II, the method used in this paper has small range error, and it can satisfy the dead reckoning accuracy requirement.

Although the step length of the pedestrians is not same, it could be seen as a constant with the average of a lot of measurement data. Lot of outdoor experiments should be carried to obtain a stable value of step length to estimate the step length indoors.

IV. OUTDOOR NAVIGATION MODE

A. Two-Dimensional Elliptical Calibration of Magnetic Sensor

The measurement error of magnetic sensor can usually be divided into the sensor error and the surrounding magnetic error. The sensor error can be thought as the device scale factor, non-orthogonal error, zero error and so on. The surrounding magnetic error can be considered as the magnetic error of the hard magnetic material and the magnetic error of the soft magnetic material [27]. In this paper, an online magnetic sensor calibration method is introduced. The error model of the magnetic sensor is set as follows:

$$H_m = \begin{bmatrix} H_{mx} \\ H_{my} \\ H_{mz} \end{bmatrix} = \begin{bmatrix} k_{11} & k_{12} & k_{13} \\ k_{21} & k_{22} & k_{23} \\ k_{31} & k_{32} & k_{33} \end{bmatrix} \begin{bmatrix} H_{tx} \\ H_{ty} \\ H_{tz} \end{bmatrix} + \begin{bmatrix} H_{x0} \\ H_{y0} \\ H_{z0} \end{bmatrix} = K H_t + H_0 \quad (8)$$

Where H_{mx}, H_{my} and H_{mz} represent the 3D (three dimensional) magnetic component under the carrier system measured by the magnetic sensor; $H_{tx}H_{ty}$ and H_{tz} represent the true3D magnetic component under the carrier system; $H_{x0}H_{y0}$ and H_{z0} are the zero offsets of the magnetic sensor. The coefficient matrix indicates the superposition of the non-orthogonal error of the magnetic sensor and the surrounding soft magnetic environment. The Magnetic sensor data correction model can be obtained as follows:

$$H_t = K^{-1}(H_m - H_0) \quad (9)$$

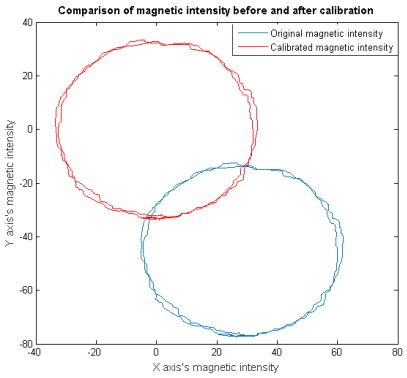

Fig. 11. Comparison of magnetic strength before and after calibration.

The modulus of the geomagnetic vector can be considered as a constant.

$$(H_t)^T H_t = const \quad (10)$$

Then,

$$(H_m - H_0)^T (K^{-1})^T (K^{-1})(H_m - H_0) = \|H_t\|^2 \quad (11)$$

The fitting equation of the ellipsoidal surface is as (12).

$$F(\xi, Z) = ax^2 + by^2 + cz^2 + 2dxy + 2exz + 2fyz + 2px + 2qy + 2rz + l = 0 \quad (12)$$

Where $\xi = [a, b, c, d, e, f, p, q, r, l]^T$ represents the parameter vector to be solved, $Z = [x^2, y^2, z^2, xy, xz, yz, x, y, z, 1]$ represents the combined vector of the measured data.

From (12), we can get:

$$(X - X_0)^T A (X - X_0) = 1 \quad (13)$$

Where

$$A = \begin{bmatrix} a & d & e \\ d & b & f \\ e & f & c \end{bmatrix}, \quad A^{-1} = \begin{bmatrix} a' & d' & e' \\ d' & b' & f' \\ e' & f' & c' \end{bmatrix}.$$

After determining the parameters, the corresponding values k_{11}, k_{22}, k_{33} and H_{x0}, H_{y0}, H_{z0} can be obtained by neglecting the small quantity. Therefore, the magnetic sensor compensation model is as:

$$\begin{bmatrix} H_{tx} \\ H_{ty} \\ H_{tz} \end{bmatrix} = \begin{bmatrix} k_{11} & & \\ & k_{22} & \\ & & k_{33} \end{bmatrix}^{-1} \left(\begin{bmatrix} H_{mx} \\ H_{my} \\ H_{mz} \end{bmatrix} - \begin{bmatrix} H_{x0} \\ H_{y0} \\ H_{z0} \end{bmatrix} \right) \quad (14)$$

The magnetic sensor calibration method is used to calibrate the magnetic sensor. The results are displayed on a two-dimensional horizontal plane in Fig. 11. The hard-magnetic coefficient H_0 and the soft magnetic coefficient K of the magnetic sensor in the horizontal can be obtained after calibration.

B. PDR/GNSS/Magnetic Sensor Outdoor Positioning Algorithm

1) Outdoor Heading Estimation: The measurement of the walking direction can be achieved through the magnetic sensor. The magnetic sensor is used to determine the absolute heading of the carrier by the magnetic measurements. The gyroscopes are commonly used as the heading angle measurement sensor. It has short-term high precision performance. In the outdoor navigation mode, the Kalman filter algorithm is often used to fuse the course of the magnetic sensor data after the two-dimensional ellipse calibration for accurate heading [28].

Choosing the magnetic heading angle ϕ as the state quantity, the Kalman filter state transition equation is as follows:

$$\phi_{\mathrm{k}} = \phi_{\mathrm{k\text{-}1}} + u_{\mathrm{k\text{-}1}} + w_{\mathrm{k}} \tag{15}$$

Where w_{k} is the white noise system. The mean of w_{k} is zero. $u_{\mathrm{k\text{-}1}}$ is the integral output the heading value, which is calculated by the gyroscope output angular rate in the sampling time, the formula is as follows:

$$u_{\mathrm{k\text{-}1}} = \int_{k-1}^{k} \omega_z dt \tag{16}$$

Where ω_z indicates the angular rate of the output of the Z-axis gyroscope.

The measurement equation of the magnetic heading ϕ_{z_k} is:

$$\phi_{z_k} = \phi_k + v_{k+1} \tag{17}$$

Where the observed noise v_k is the white noise and the coefficient matrix of the Kalman filter is: $\mathrm{F} = \mathrm{G} = \mathrm{H} = 1$.

2) Outdoor Location Estimation: The personal inertial positioning method can meet the needs of the personal positioning and achieve personal positioning under GNSS-denied environment, but the positioning results will still diverge with the time or walking distance. As GNSS positioning results will not diverge with the walking time or walking distance. The personal mobile positioning is the preferred personal mobile positioning program when GNSS is available [29]. It can guarantee the effectiveness of the positioning results.

The Samsung S6 smartphone is used in GNSS test. This smartphone is a small-size and stable-performance devices, which can provide the effective positioning results at most of the time in the case of the GNSS signal can be obtained. Lots of the data are analyzed to determine the validity of the GNSS positioning results. The NMEA (National Marine Electronics Association) format navigation information output is supplied by the module, which contains the information such as the number of the visible satellites, the latitude, the longitude and so on.

The experiments of satellite positioning performance were carried out in an open outdoor environment. After walking a circle in the open playground, the experimental satellite positioning results can be seen in Fig. 12, Fig 13, Fig 14 and Fig 15. Considering the multi-path errors by the high-rise buildings, when the number of the working satellites is less than 4, there are lots of errors in positioning results. The HDOP value and the number of visible satellites are used to judge whether the GPS signal is available or not. It is widely considered that when the number of visible satellites remains above 4 and the HDOP value is less than 3, the satellite positioning results is available.

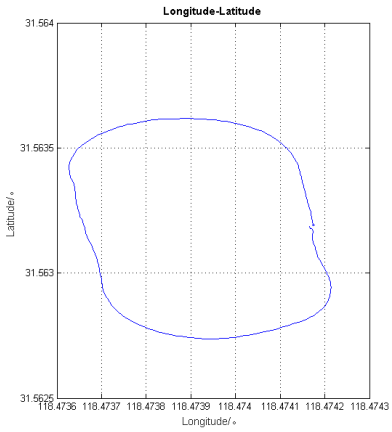

Fig. 12. Latitude and longitude of satellite positioning.

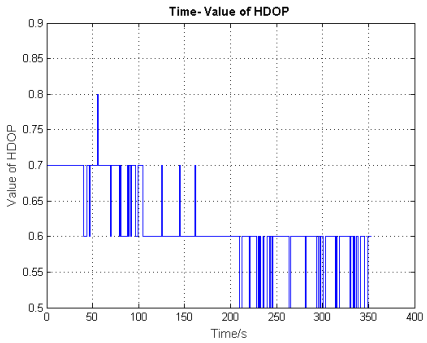

Fig. 13. GPS horizontal position precision factor.

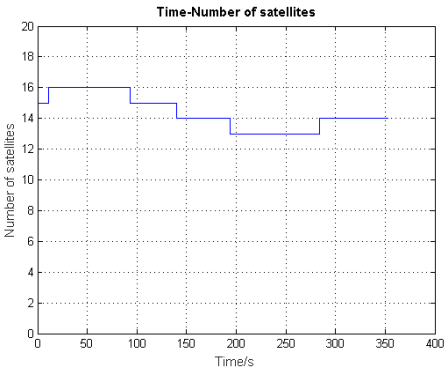

Fig. 14. GPS visible satellites.

The magnetic sensor in the system can provide an accurate heading angle measurement. The satellite navigation system can provide an effective position measurement. Therefore, the magnetic heading angle and the GNSS position can be the measurements by the Kalman filter. The state vector of the system filtering is listed as:

$$\boldsymbol{X} = [E N P \varphi]^T \tag{18}$$

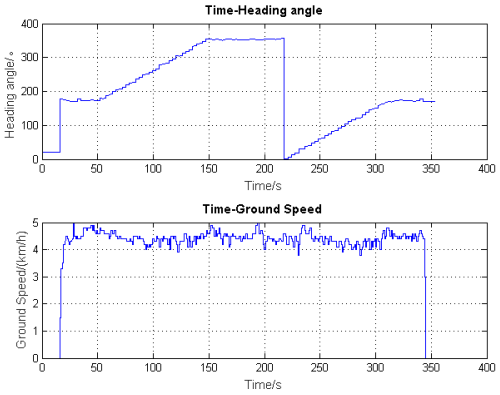

Fig. 15. Heading and speed of satellite positioning.

Where E, N respectively is the east coordinates and north coordinates of PDR in the northeast coordinate system; P is the step length; φ is the heading angle.

The observation vector is:

$$Z = [Z_{GPS} \quad Z_{PDR}]^T \tag{19}$$

Where $Z_{GPS} = [E_{GPS} N_{GPS}]$ is the east and north position of the GNSS output. $Z_{PDR} = [P_{PDR} \varphi_{PDR}]$ is the step length after GNSS calibration and the heading after magnetic sensor calibration.

The equation of the state is as follows:

$$\begin{cases} E_{K+1} = E_K + P_K \cdot \sin\varphi_k + w_E \\ N_{K+1} = N_K + P_K \cdot \cos\varphi_k + w_N \\ P_{K+1} = P_K + w_p \\ \varphi_{K+1} = \varphi_K + w_\varphi \end{cases} \tag{20}$$

Where $w_k = [\, w_E \;\; w_N \;\; w_p \;\; w_\varphi \,]^T$ is the white noise of the navigation system.

The measurement equation is:

$$\begin{aligned} Z_{k+1} &= H_{k+1} X_{k+1} + v_{k+1} \\ &= \begin{bmatrix} 1 & 0 & 0 & 0 \\ 0 & 1 & 0 & 0 \\ 0 & 0 & 1 & 0 \\ 0 & 0 & 0 & 1 \end{bmatrix} X_{k+1} + v_{k+1} \end{aligned} \tag{21}$$

Where, the observation noise v_k is white noise. H_k is the observation coefficient matrix, Z_k is the observation.

The state equation is a nonlinear system. According to the extended Kalman filter principle, the state transition matrix is:

$$\phi_{k+1} \approx \left.\frac{\partial f_k}{\partial \mathrm{X}}\right|_{X=\bar{X}_K} = \left[\begin{matrix} 1 & 0 & \sin\varphi & P\cos\varphi \\ 0 & 1 & \cos\varphi & -P\sin\varphi \\ 0 & 0 & 1 & 0 \\ 0 & 0 & 0 & 1 \end{matrix}\right]\Bigg|_{X=\bar{X}_K} \tag{22}$$

3) Positioning Experiment Based on PDR/Magnetic/Satellite Information Fusion: In order to verify the proposed optimization algorithm based on the magnetic sensor, the smartphone is held on the hand horizontally to collect the walking data around the playground of Nanjing University of Aeronautics and Astronautics. The IMU, the magnetic sensors, the satellite receiver module and other modules of the smartphone are turned on together to collect the data. The output frequency of IMU and the magnetic sensor is 50Hz. The frequency of navigation result of the GNSS module is 1Hz. The experimental travel route is shown in Fig. 16.

Fig. 16. Experimental roadmap.

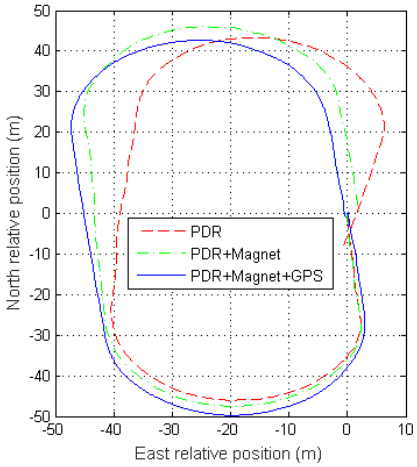

Fig. 17. Three kinds of the pedestrian positioning experiment result.

TABLE III
POSITIONING ERROR COMPARISON TABLE BEFORE AND AFTER SATELLITE/MAGNETIC SENSOR FUSION

Used sensors	Position error	Percentage of error
Pure inertial PDR	15.6m	3.90%
Magnetic sensor + PDR	3.46m	0.87%
Heading KF	1.72m	0.44%
GNSS + Magnetic sensor + PDR	0.95m	0.23%

The result of pure inertial navigation, magnetic sensor auxiliary result and satellite/magnetic fusion result are compared in Fig. 17. After a long-distance walk, the pure inertial navigation result shows the heading drift obviously. With the assistant of the magnetic sensor, the heading drift of the navigation has been greatly reduced. When GNSS is introduced into the

position algorithm, the pedestrian positioning result is further improved comparing to the other two methods. Therefore, in the satellite navigation available area, the introduction of satellite navigation can effectively improve the positioning performance of the system. In the case of long distance walking, the inertial position accuracy can be effectively improved.

The errors of three kinds of the positioning methods are shown in Table III. In outdoor long-distance walking, pure inertial positioning error of smartphone sensors is more than 15 m, which is 3.9% of the total walking distance. The position error after using the calibrated magnetic heading is about 3.5 m, which is 0.87% of the total travel distance. It is indicated that the magnetic sensor can be used to assist the position and improve the heading accuracy when the satellite signal is available. After the calibration, the magnetic heading and the gyro integral heading are used together for the Kalman filter, and the error is 1.72 m, which is 0.68% of the distance. When the satellite signal is added into the system, the positioning error is reduced to 0.95m, accounting for 0.23% of the total walking distance. It can be seen that the algorithm proposed in this paper can effectively improve the accuracy of pedestrian positioning.

V. Smartphone Seamless Position System Design

The smartphone positioning real time software is realized in Android intelligent terminal. To realize the seamless navigation, the indoor map is added to the Baidu Map. The position database is established.

A. Secondary Development of Baidu Map

To realize the indoor positioning on the smartphone, the indoor map must be presented on the smartphone. The indoor map mentioned in this paper is the 5th floor of the CAE (College of Automation Engineering), NUAA. The two buildings of the CAE are connected by the passageways. The task consists of the following steps:

1) Got the profile of the floor and the relative position of the room
   The distance is measured by the laser range finder, which error is about 1 millimeter. To simplify the map, there are three important points are as follows:
   a. Using the room number to get the position information of the room.
   b. Ignoring the thickness of the wall of the building.
   c. The layout of the rooms is simplified as the rectangles.
2) Differential GNSS information collection
   The differential GNSS information was collected to measure the edges of the building; the room size can be calculated on average.
3) Baidu Map layer cover
   As shown in Fig. 18, the cover layer is completed through the customized geometry demo, including the polygon, lines and words.

B. Design of Smartphone Position Software

The designed target of the software is to develop a platform to complete the functions, such as the sensors reading, real-time calculation. As in Fig. 19, the platform can save the data from sensors and the navigation result. It is very convenient for the post processing.

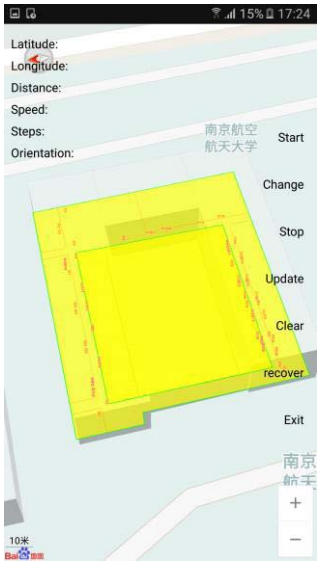

Fig. 18. Indoor map layer shown inside Baidu Map.

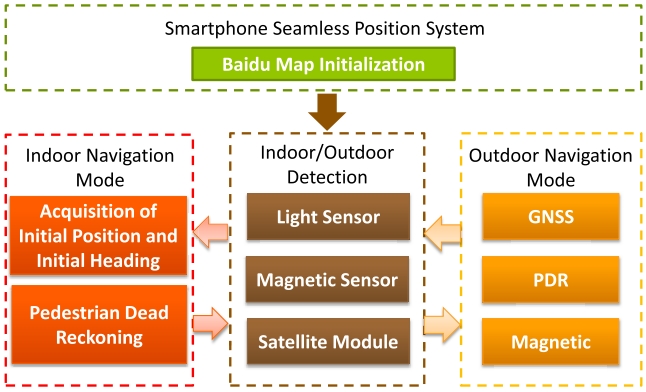

Fig. 19. Framework of the software platform.

TABLE IV
Comparison of Indoor Positioning Results

Navigation mode	Last position error	Percent of distance(295.5m)
GPS identification	6.96m	2.36%
Comprehensive identification	3.16m	1.07%

VI. Experiment and Analysis

To test the availability of the seamless navigation system proposed in this paper, a long-time walking experiment is completed in Jiangning Campus, Nanjing University of Aeronautics and Astronautics. The smartphone is held in the hand. The trajectory is shown in Fig. 20. The experimental route areas include the indoor/outdoor environments.

Two kinds of algorithms are compared in Fig. 21. The blue point line is the indoor/outdoor detection result relying on the GNSS only. In the critical semi-open area, the GNSS signal is weak and the position error can be up to 10m.

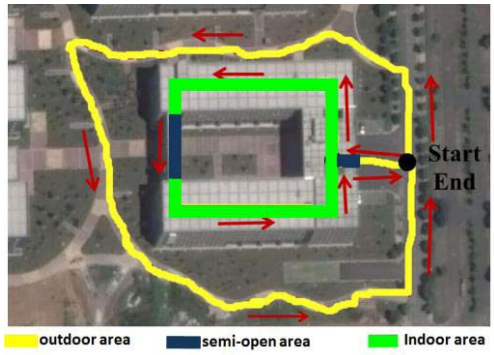

Fig. 20. Trajectory of the walking experiment.

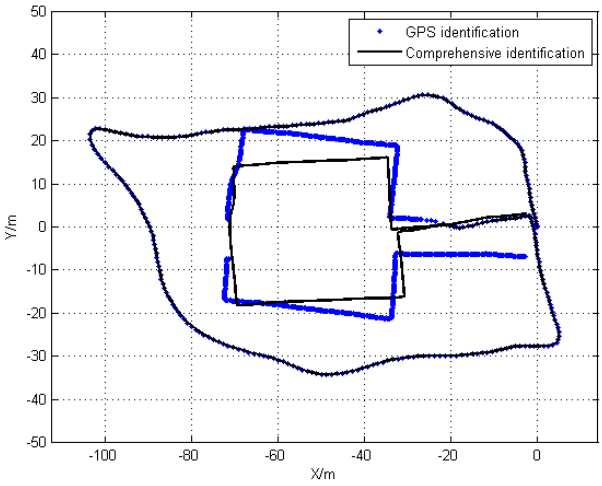

Fig. 21. Results of two kinds of identifications.

Fig. 22. Navigation result on the smartphone.

The black line is the indoor/outdoor detection result relying on the comprehensive judgment of the light sensor, the magnetic sensor and the GNSS. This method can clearly determine the proper status when the smartphone is in the semi-open area. The indoor positioning mode can be used to remove the abnormal effects of GNSS. This strategy is very helpful to improve the overall accuracy of the positioning. As shown in Table IV, the accuracy of the indoor positioning increased by 55%.

The navigation result displayed with the smartphone software proposed in the paper is shown in Fig. 22. It can be seen that the navigation results can fit the pedestrian trajectory of the building properly.

VII. Conclusions

A smartphone fusion location method optimized by the indoor/outdoor detection is proposed in the paper. The experiment results indicate that this method can effectively improve the continuity and the accuracy of the indoor/outdoor seamless position.

The light sensor, the magnetic sensor and the satellite signal is integrated together to identify the indoor/outdoor status. When the device is detected indoors, Pedestrian Dead Reckoning algorithm based on the MEMS accelerometers and the gyroscopes is used. The indoor electronic map is added to realize the seamless connection of the indoor/outdoor geographic information, which can be used to determine the position and the heading of the moving course. When the device is detected outdoors, the GNSS and the magnetic sensor are introduced into the system to assist the inertial navigation system.

The corresponding android software has been realized in the Samsung S6 smartphone. The software can be applied to any other android smartphones.

To improve the accuracy of the dead reckoning algorithm indoors is the most important part. We try to meet the complicated requirements of long-time and long-distance indoor navigation, which will be helpful to achieve a reliable pedestrian navigation without attitude constraint in the future.

References

[1] J. Liu, R. Chen, L. Pei, R. Guinness, and H. Kuusniemi, "A hybrid smartphone indoor positioning solution for mobile LBS," *Sensors*, vol. 12, no. 12, pp. 17208–17233, 2012.

[2] Y. Zhuang, H. Lan, Y. Li, and N. El-Sheimy, "PDR/INS/WiFi integration based on handheld devices for indoor pedestrian navigation," *Micromachines*, vol. 6, no. 6, pp. 793–812, 2015.

[3] W. Kang and Y. Han, "SmartPDR: Smartphone-based pedestrian dead reckoning for indoor localization," *IEEE Sensors J.*, vol. 15, no. 5, pp. 2906–2916, May 2015.

[4] M. M. Saad, C. J. Bleakley, T. Ballal, and S. Dobson, "High-accuracy reference-free ultrasonic location estimation," *IEEE Trans. Instrum. Meas.*, vol. 61, no. 6, pp. 1561–1570, Jun. 2012.

[5] H. Leppäkoski, J. Collin, and J. Takala, "Pedestrian navigation based on inertial sensors, indoor map, and WLAN signals," *J. Signal Process. Syst.*, vol. 71, no. 3, pp. 287–296, 2013.

[6] Y. Noh, H. Yamaguchi, and U. Lee, "Infrastructure-free collaborative indoor positioning scheme for time-critical team operations," *IEEE Trans. Syst., Man, Cybern., Syst.*, to be published.

[7] W. Chen, R. Chen, Y. Chen, H. Kuusniemi, and J. Wang, "An effective pedestrian dead reckoning algorithm using a unified heading error model," in *Proc. IEEE/ION Position Location Navigat. Symp. (PLANS)*, May 2010, pp. 340–347.

[8] Y. Li, Z. He, and J. Nielsen, "Enhancing Wi-Fi based indoor pedestrian dead reckoning with security cameras," in *Proc. 4th Int. Conf. IEEE Ubiquitous Positioning, Indoor Navigat. Location Based Serv. (UPINLBS)*, Nov. 2016, pp. 107–112.

[9] L.-H. Chen, E. H.-K. Wu, M.-H. Jin, and G.-H. Chen, "Intelligent fusion of Wi-Fi and inertial sensor-based positioning systems for indoor pedestrian navigation," *IEEE Sensors J.*, vol. 14, no. 11, pp. 4034–4042, Nov. 2014.

[10] S. He and S.-H. G. Chan, "Wi-Fi fingerprint-based indoor positioning: Recent advances and comparisons," *IEEE Commun. Surveys Tuts.*, vol. 18, no. 1, pp. 466–490, 1st Quart., 2016.
[11] W. Seo, S. Hwang, and J.-M. Lee, "Precise outdoor localization with a GPS–INS integration system," *Robotica*, vol. 31, no. 31, pp. 371–379, 2013.
[12] L. Zhong *et al.*, "Dynamic compensation filter algorithm for INS/SFGPS-PPP tightly coupled system," *Chin. J. Sci. Instrum.*, vol. 37, no. 6, pp. 1283–1289, 2016.
[13] J. Cheng, L. Yang, Y. Li, and W. Zhang, "Seamless outdoor/indoor navigation with WIFI/GPS aided low cost inertial navigation system," *Phys. Commun.*, vol. 13, pp. 31–43, Dec. 2014.
[14] Y. Sakamoto, T. Ebinuma, K. Fujii, and S. Sugano, "GPS-compatible indoor-positioning methods for indoor-outdoor seamless robot navigation," in *Proc. IEEE Workshop Adv. Robot. Soc. Impacts (ARSO)*, May 2012, pp. 95–100.
[15] O. Canovas, P. E. Lopez-de-Teruel, and A. Ruiz, "Detecting indoor/outdoor places using WiFi signals and AdaBoost," *IEEE Sensors J.*, vol. 17, no. 5, pp. 1443–1453, Mar. 2017.
[16] A. Kealy, G. Roberts, and G. Retscher, "Evaluating the performance of low cost MEMS inertial sensors for seamless indoor/outdoor navigation," in *Proc. IEEE/ION Position Location Navigat. Symp. (PLANS)*, May 2010, pp. 157–167.
[17] A. Kealy, G. Retsche, D. Grejner-Brzezinska, V. Gikas, and G. Roberts, "Evaluating the performance of MEMS based inertial navigation sensors for land mobile applications," *Arch. Photogram.*, vol. 22, pp. 237–248, Dec. 2011.
[18] V. Radu, P. Katsikouli, R. Sarkar, and M. K. Marina, "A semi-supervised learning approach for robust indoor-outdoor detection with smartphones," in *Proc. 12th ACM Conf. Embedded Netw. Sensor Syst.*, 2014, pp. 280–294.
[19] X. Chen, Y. Xu, Q. Li, J. Tang, and C. Shen, "Improving ultrasonic-based seamless navigation for indoor mobile robots utilizing EKF and LS-SVM," *Measurement*, vol. 92, pp. 243–251, Oct. 2016.
[20] M. Li, P. Zhou, Y. Zheng, Z. Li, and G. Shen, "IODetector: A generic service for indoor/outdoor detection," *ACM Trans. Sensor Netw.*, vol. 11, no. 2, 2015, Art. no. 28.
[21] M. Okamoto and C. Chen, "Improving GPS-based indoor-outdoor detection with moving direction information from smartphone," in *Proc. ACM Int. Symp. Wearable Comput.*, 2015, pp. 257–260.
[22] Y. Kim, S. Lee, S. Lee, and H. Cha, "A GPS sensing strategy for accurate and energy-efficient outdoor-to-indoor handover in seamless localization systems," *Mobile Inf. Syst.*, vol. 8, no. 4, pp. 315–332, 2014.
[23] R. Harle, "A survey of indoor inertial positioning systems for pedestrians," *IEEE Commun. Surveys Tuts.*, vol. 15, no. 3, pp. 1281–1293, 3rd Quart., 2013.
[24] V. Renaudin and C. Combettes, "Magnetic, acceleration fields and gyroscope quaternion (MAGYQ)-based attitude estimation with smartphone sensors for indoor pedestrian navigation," *Sensors*, 14, no. 12, pp. 22864–22890, 2014.
[25] J. Z. Flores and R. Farcy, "Indoor navigation system for the visually impaired using one inertial measurement unit (IMU) and barometer to guide in the subway stations and commercial centers," in *Proc. Int. Conf. Comput. Handicapped Pers.*, 2014, pp. 411–418.
[26] A. R. Jimenez, F. Seco, C. Prieto, and J. Guevara, "A comparison of pedestrian dead-reckoning algorithms using a low-cost MEMS IMU," in *Proc. IEEE Int. Symp. Intell. Signal Process.*, Aug. 2009, pp. 37–42.
[27] Z. Liu, L. Zhang, Q. Liu, Y. Yin, L. Cheng, and R. Zimmermann, "Fusion of magnetic and visual sensors for indoor localization: Infrastructure-free and more effective," *IEEE Trans. Multimedia*, vol. 19, no. 4, pp. 874–888, Apr. 2016.
[28] S.-D. Bao, X.-L. Meng, W. Xiao, and Z.-Q. Zhang, "Fusion of inertial/magnetic sensor measurements and map information for pedestrian tracking," *Sensors*, vol. 17, no. 2, p. 340, 2017.
[29] L. T. Hsu, Y. Gu, Y. Huang, and S. Kamijo, "Urban pedestrian navigation using smartphone-based dead reckoning and 3-D map-aided GNSS," *IEEE Sensors J.*, vol. 16, no. 5, pp. 1281–1293, Mar. 2016.

Qinghua Zeng received the Ph.D. degree from the College of Automatic Engineering (CAE), Nanjing University of Aeronautics and Astronautics (NUAA), Nanjing, China, in 2006. He is currently an Associate Professor with the CAE, NUAA, and an academic of the Chinese Society of Inertial Technology, the Chinese Society of Astronautics, the IAENG, and the IEEE. His research interests include seamless positioning, integrated navigation and multi-sensor information fusion.

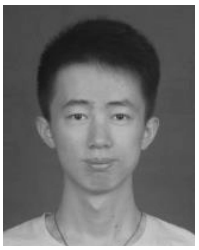

Jingxian Wang received the B.S. degree from the Nanjing University of Aeronautics and Astronautics (NUAA), Nanjing, China, in 2015. He is currently pursuing the M.S. degree with the Navigation Research Center, College of Automatic Engineering, NUAA. His research interests include multi-information fusion, indoor positioning, and navigation.

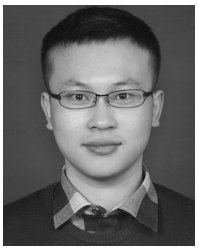

Qian Meng received B.S. degree from Nanjing University of Aeronautics and Astronautics (NUAA), Nanjing, China, in 2013. He is currently pursuing the Ph.D. with NUAA. He is an academic of the Chinese Society of Inertial Technology. His research focuses on the GNSS software-defined receiver and INS/GNSS Integrated navigation.

Xiaoxue Zhang received the B.S. and M.S. degrees from the Nanjing University of Aeronautics and Astronautics, Nanjing, China, in 2014 and 2017, respectively. She is currently with Lenovo as an Android Software Developer.

Shijie Zeng received the B.S. degree from the Nanjing University of Aeronautics and Astronautics (NUAA), Nanjing, China, in 2016. He is currently pursuing the M.S. degree with the Navigation Research Center, College of Automatic Engineering, NUAA. His research interests include pedestrian navigation, indoor position, and integrated navigation.